

## Reconstruction of standard and inverse vector fields equivalent to a Rössler system

G. Gouesbet

*Laboratoire d'Energétique des Systèmes et Procédés, Institut National des Sciences Appliquées de Rouen,  
Boîte Postale 08, 76131, Mont-Saint-Aignan CEDEX, France*

(Received 21 February 1991; revised manuscript received 21 May 1991)

Ordinary differential equations of continuous dynamical systems, or at least of equivalent systems, can be reconstructed from numerical scalar time series. Methods are exemplified for a Rössler band. Equivalent systems are standard and inverse systems, which are systematically investigated. Validations rely (i) qualitatively on comparisons between phase portraits and (ii) quantitatively on comparisons between generalized dimension spectra. By-products of the work are an information-compression scheme for time-series encoding and the introduction of squeezed systems that facilitate evaluations of generalized dimensions of small order  $q < 1$ .

PACS number(s): 05.45.+b, 47.10.+g, 05.40.+j

### I. INTRODUCTION

Current methods to evaluate attractor invariants from numerical scalar time series, such as generalized dimensions  $D_q$  and generalized entropies  $K_q$ , rely on Takens's theorem and criteria [1,2], and require the reconstruction of attractors in phase spaces of dimension  $n$  generically much larger than a minimal dimension  $n_0$ . When the algorithms are successful, there is little doubt that they provide us with valuable information. For instance, we may have definitely concluded that the system is deterministic and evaluated the effective number of degrees of freedom required to describe the dynamics telling us how many ordinary differential equations we need to produce a phenomenological model of the system. But the applied scientist would feel disappointed by the limited interest of such information and, after having determined a spectrum of generalized dimensions, he would ask: what is to be done now? Actually, the applied scientist would be most interested if, besides the evaluation of invariants, the available numerical scalar time series would automatically allow for the construction of phenomenological models themselves, i.e., for the reconstruction of vector fields equivalent to the original ones. The meaning of the word equivalent is later discussed when appropriate. This paper is devoted to this vector-field reconstruction problem.

Since our methods are exemplified in a rather simple case, we clearly expect that variants will be produced in the future and that they will be in fact needed to investigate more and more complicated situations. We expect, however, that most of the essential ideas will be preserved. We shall also distinguish between what is particular to the studied example and therefore should be generalized to attack more difficult cases, making possible suggestions for these generalizations, and what is expected to be robust. We also mention that, during the reviewing process of this paper, a similar work has been successfully carried out for the Lorenz system [3]. Actually, we believe that our methods possess a fair degree of generality, as discussed in Sec. II. A, in which we explain for

which kinds of problems we may expect the existence of so-called standard systems.

Concerning precursors, Packard *et al.* mentioned that Rössler equations "are sufficiently simple that one can explicitly obtain a new set of three ordinary differential equations describing the dynamics of the state space comprised of a coordinate along with its first and second derivatives" (Ref. [4], p. 714) and use this idea to evaluate a characteristic exponent. From this lapidary statement, we inferred, maybe incorrectly, that the authors had in mind the vector-field reconstruction problem. In any case, no systematic development of the idea was given. Later on, Cremers and Hübler [5] provide a more systematic discussion of the same idea and consider the case of a Lorenz system with chaotic dynamics and of a van der Pol oscillator with periodic motion. In both cases, assessment of the quality of the model is based on a comparison between the parameters of the original differential equations with the parameters recovered from the time series. Such a criterion of quality is, however, insufficient, as discussed in Ref. [6], because small errors in parameter values may even destroy the attractor in relation with the concept of structural stability, depending also on the proximity of bifurcation loci. Therefore, the only convincing validation of the presented methods in our opinion relies on the successful determination of a limit-cycle radius for a van der Pol periodic motion. We developed our own ideas for the first time in Ref. [6], investigating a strange chaotic attractor generated by Rössler equations. We introduced standard systems that are used to numerically evaluate a set of constants associated with reconstructed vector fields. Standard systems (SS's) are available even when the original vector field is unknown. However, validations of the quality of our reconstructions were examined by qualitatively and quantitatively studying so-called inverse standard systems. When the original vector field is unknown, these inverse standard systems are also unknown. Therefore, this paper concentrates on the study of standard systems and inverse nonstandard systems, all of them being known even when the original vector field is unknown. Reference [6]

contains more introductory material and also some various discussions that are not repeated here, where we focus on new results.

The paper is organized as follows. Section II introduces the standard systems, the standard transformations linking them to original systems (when they are known), and some of their properties, and also the methods of reconstruction producing a set of reconstructed constants defining the reconstructed vector fields. Section III is devoted to the numerical study of standard systems. Section IV is devoted to the definition and numerical study of several inverse systems. Validations of our reconstructions rely on comparisons between phase portraits and computations of generalized dimensions. An extensive discussion of the comparisons between generalized dimension spectra is provided in Sec. V. Section VI is a conclusion in which we also mention the next steps to accomplish before vector-field reconstructions can be applied to noisy experimental systems.

## II. STANDARD SYSTEMS, TRANSFORMATIONS, AND RECONSTRUCTION METHODS

### A. The system under study

We consider the example of a Rössler band generated by the following equations:

$$\dot{x} = -y - z, \quad (1)$$

$$\dot{y} = x + ay, \quad (2)$$

$$\dot{z} = b + z(x - c), \quad (3)$$

with control parameter values  $a = 0.398$ ,  $b = 2$ , and  $c = 4$ , for which the asymptotic motion settles down on a strange chaotic attractor [7]. Rössler equations are particularly simple, displaying only one nonlinear vector-field component, and therefore provide us with an easy opportunity to illustrate basic methods. We also choose the case of a chaotic attractor, which represents the most interesting issue to investigate. The system described by (1)–(3) is called the original system (OS). In many cases, especially for experimental systems, the OS is unknown.

### B. Standard systems

We assume that our knowledge of the OS is contained in a recorded numerical scalar time series  $\{x_i\}$ , i.e., we give to variable  $x$  a special status without any loss of generality. Standard systems (SS's) are then defined by

$$\dot{x} = Y, \quad (4)$$

$$\dot{Y} = Z, \quad (5)$$

$$\dot{Z} = F(x, Y, Z). \quad (6)$$

The number of equations of the SS's is equal to the number of equations  $n_0$  of the OS. When the OS is unknown, a preliminary step therefore requires a prior evaluation of the number of degrees of freedom of the system from series  $\{x_i\}$ . This issue is discussed in Ref. [6]. We would, however, like to stress the relation between this

problem and Takens's theorem. We consider a strange attractor of typical fractal dimension  $D$  embedded in a minimal phase space of dimension  $n_0$  (then  $D \leq n_0$ ). Takens's theorem states that the attractor may be generically reconstructed in a phase space of dimension  $n \geq n_T$  in which  $n_T = 2D + 1$  (ideally,  $D$  would refer to the Hausdorff dimension of the set). Loosely speaking, the word generically here means that using  $n \geq n_T$  is always sufficient to reconstruct the attractor. This theorem is used for numerical calculations of invariants, with, for instance, the time-delay method, by studying reconstructed attractors diffeomorphically related to the OS. Of course, reconstruction phase spaces of dimension  $n < n_T$  may also work. In particular, vector-field reconstructions discussed in this paper use a minimal phase space of dimension  $n_0$ . For a heuristic discussion, see Parker and Chua (Ref. [8], Sec. 7.2).

We remark that standard coordinates  $(x, Y, Z)$  use  $(n_0 - 1)$  derivatives of the recorded scalar variable  $x$ . However, due to the left-hand side of Eq. (6), the  $n_0$ th derivative  $\dot{Z}$  is also involved in the problem. Not all continuous systems defined by vector fields possess standard forms. For instance, we may consider the rather uninteresting trivial case  $\dot{x} = f(x)$ ,  $\dot{y} = g(y)$  in  $\mathbb{R}^2$ . Due to the uncoupling between variables  $x$  and  $y$ , this system does not own any standard form. Conversely, the set of dynamical systems owning standard forms is not empty. This set contains all the examples we have studied or are currently studying, i.e., the Rössler system [6], the Lorenz system [3] and also a three-dimensional (3D) vector field produced by a simple model of thermal lens oscillations described in Ref. [9]. Following a discussion by Parker and Chua (Ref. [8], p. 193), to identify uniquely a trajectory of an  $n$ th-order system,  $n$  independent pieces of information are required. As above, they may be  $n$  successive derivatives including the zeroth derivative, i.e.,  $x$  itself. This method works whenever the state equation can be transformed into a single  $n$ th-order scalar differential equation, i.e., it works generically but fails when variables are not sufficiently coupled, as in the aforementioned example. Parker and Chua also comment that another classical way of specifying a trajectory by giving  $n$  samples of the  $j$ th component of the state (time-delay method) involves only one component of the state, as does the use of derivatives, and therefore also fails in the case of insufficient coupling between variables, but works generically. Furthermore, it is known that the time-delay method and the use of derivatives are topologically equivalent. Consequently, we believe that the class of systems owning standard forms is very large, although our heuristic discussion should later be given a more formal basis. We readily establish that the standard exact system (SES) corresponding to the OS reads

$$\begin{aligned} \dot{Z} = & ab - cx + x^2 - axY + xZ + (ac - 1)Y + (a - c)Z \\ & - \frac{Y}{a + c - x}(x + b - aY + Z), \end{aligned} \quad (7)$$

in which only the third equation is given. Note the existence of a (seemingly) singular term at  $x_c = (a + c)$ , to be discussed later.

### C. Standard transformations

The direct standard transformation (DST) expresses the standard coordinates  $(x, Y, Z)$  versus the original coordinates  $(x, y, z)$ . For the Rössler system, the DST reads

$$x = x, \quad (8)$$

$$Y = -y - z, \quad (9)$$

$$Z = -b - x - ay + z(c - x). \quad (10)$$

Conversely, the inverse standard transformation (IST) expresses original coordinates versus standard ones. For the Rössler system, we obtain

$$x = x, \quad (11)$$

$$y = -\frac{Y(c - x) + Z + b + x}{a + c - x}, \quad (12)$$

$$z = \frac{Z + b + x - aY}{a + c - x}. \quad (13)$$

Clearly, (11)–(13) are only valid when  $x$  is not equal to a critical  $x_c = (a + c)$  also appearing in the (seemingly) singular term of (7). Specifying  $x = x_c$  in the DST (8)–(10), we establish the following facts.

(i) At  $x = x_c$ , standard coordinates are related by the relation

$$aY - Z = (a + b + c). \quad (14)$$

(ii) The transformation at  $x = x_c$  is not invertible. The best we can obtain is the trivial relation  $x = x$  and

$$y + z = -Y = \frac{-(a + b + c + Z)}{a}, \quad (15)$$

that is to say there is no way to express  $y$  and  $z$  independently.

We also establish that, when  $x \rightarrow x_c$ , relation (7) for  $\dot{Z}$  leads to

$$\dot{Z} \rightarrow -Y(1 + z) + aZ. \quad (16)$$

Since  $z$ ,  $Y$ , and  $Z$  are bounded, Eq. (16) evidences that Eq. (7) is actually not singular at  $x = x_c$ . The (seemingly) singular term in (7) is therefore called a pseudosingular term. However, due to the lack of invertibility at the critical  $x_c$  locations, we cannot express  $z$  ( $x, Y, Z$ ) and therefore numerical integration of (7) at the critical locations is impossible. Numerical consequences and other complementary discussions of this problem will be provided later when appropriate. For now, just note that the set of points  $\{x = x_c\}$  in the phase space  $(x, Y, Z)$  has a Lebesgue measure equal to 0. Because numerical integrations rely on discrete schemes, the probability of landing on a critical location during the integration process is also equal to 0, i.e., integration is permitted almost everywhere. We also emphasize that, when the OS is unknown, DST and IST are also unknown, which, however, does not preclude the knowledge of SS's.

### D. DST properties

In this subsection, we examine how the original phase-space structure is mapped to the standard phase space by the DST. Many results have been obtained using symbolic computations with the aid of the software MAPLE.

The Rössler system (OS) owns two fixed points  $P_{OS}^1$  and  $P_{OS}^2$  defined by coordinates  $(x_1, y_1, z_1)$  and  $(x_2, y_2, z_2)$ , respectively, given as

$$z_{1,2} = \frac{c \mp (c^2 - 4ab)^{1/2}}{2a}, \quad (17)$$

$$y_{1,2} = -z_{1,2}, \quad (18)$$

$$x_{1,2} = az_{1,2}, \quad (19)$$

in which signs  $(-)$  and  $(+)$  in (17) correspond to  $z_1$  and  $z_2$ , respectively.  $P_{OS}^1$  is located near the coordinate center (inner fixed point), while  $P_{OS}^2$  is located far from it and also far outside of the attractor (the outer fixed point). Writing the Jacobian of the OS, then evaluating eigenvalues, we determine the stability type of the fixed points.  $P_{OS}^1$  owns one negative real eigenvalue associated with a one-dimensional stable manifold, and two complex conjugate eigenvalues with positive real parts, associated with a two-dimensional unstable manifold in which trajectories are spiralling outwards, i.e.,  $P_{OS}^1$  is a saddle focus. Similarly,  $P_{OS}^2$  is also a saddle focus. However, the real eigenvalue is now positive, generating a one-dimensional unstable manifold, and the two complex conjugate eigenvalues have negative real parts, generating a two-dimensional stable manifold.

The two fixed points  $P_{OS}^1$  and  $P_{OS}^2$  of the OS are mapped by the DST to the two fixed points  $P_{SES}^1$  and  $P_{SES}^2$  of the SES, respectively. Applying the DST to  $P_{OS}^1$  and  $P_{OS}^2$  coordinates, or also setting the vector field of the SES to zero, locations of  $P_{SES}^1$  and  $P_{SES}^2$  are found to be

$$x_{1,2} = \frac{c \mp (c^2 - 4ab)^{1/2}}{2}, \quad (20)$$

$$Y_{1,2} = Z_{1,2} = 0, \quad (21)$$

in which, again, signs  $(-)$  and  $(+)$  in (20) correspond to  $x_1$  and  $x_2$ , respectively. Therefore, both fixed points now lie on the  $x$  axis. Fixed points near and far away from the coordinate center in the original phase space are mapped to fixed points near and far away from the coordinate center in the standard phase space. We also show that the eigenvalue characteristic equations of the OS and SES are strictly equivalent. Therefore, DST preserves (i) the number of fixed points, and (ii) their eigenvalues and stability types.

We now consider the attractor  $A_{OS}$  generated by the OS. It is mapped by the DST to an object  $A_{SES}$  of the SES. Since the DST does not contain any singularity,  $A_{SES}$  is a well-defined object. This point heuristically confirms that there is no singularity in Eq. (7) because integrating the SES must generate the object  $A_{SES}$  (as we shall actually be able to do). We now comment that  $A_{SES}$  must be an attractor in agreement with numerical checks obtained by taking initial conditions far away from  $A_{SES}$ .

Consider a point  $P_{OS}$  in the basin of attraction of  $A_{OS}$ , far away from it. The trajectory  $L_{OS}$  starting from  $P_{OS}$  asymptotically approaches  $A_{OS}$ .  $P_{OS}$  is mapped by the DST to a point  $P_{SES}$  far away from the object  $A_{SES}$ . Similarly, the trajectory  $L_{OS}$  is mapped to a trajectory  $L_{SES}$  starting from  $P_{SES}$ . Since any point of the attractor  $A_{OS}$  is mapped to a point in the object  $A_{SES}$ , we deduce that the trajectory  $L_{SES}$  asymptotically approaches  $A_{SES}$ , which is therefore an attractor. Then, the DST also preserves the stability properties of  $A_{OS}$ .

The DST also preserves pseudoperiod values. This has been numerically checked and may be established as follows. The pseudoperiod  $T_{0,OS}$  of  $A_{OS}$  is defined by choosing special well-defined events  $E_{i,OS}$  on the trajectory. In practice, for the Rössler system,  $E_{i,OS}$  is defined by successive passing of the trajectory through a maximum of the coordinate  $z$  (see Fig. 5 and Sec. IV A) occurring at successive dates  $t_i$ . The pseudoperiod is calculated as the average of many successive return times  $(t_{i+1} - t_i)$ , which are equal to  $\lim_{\delta t \rightarrow 0} (N_{i+1} - N_i) \delta t$ , in which  $\delta t$  is the time step of the integration algorithm and  $N_i$  is the number of time steps to reach the  $i$ th event. The DST maps events  $E_{i,OS}$  to events  $E_{i,SES}$  to be used to evaluate the pseudoperiod  $T_{0,SES}$  of the attractor  $A_{SES}$ . Integrating OS and SES with the same time step, each point at the  $N_i$ th step on  $A_{OS}$  is mapped to a unique point at the same time step on  $A_{SES}$ . We therefore conclude that successive return dates  $t_i$  to meet  $E_{i,OS}$  in OS and  $E_{i,SES}$  in SES are equal, hence  $T_{0,OS} \equiv T_{0,SES}$ . More generally, we similarly show that all attractors to be considered in this paper own the same pseudoperiod noted  $T_0$ , numerically found to be equal to 6.22.

We now come to properties that are not preserved by the DST. The first one is the distance between fixed points. From (17)–(21), we find that the Euclidean distances  $D_{OS}$  and  $D_{SES}$  of the fixed points of the OS and the SES are equal to, respectively,

$$D_{OS} = \left[ \left( 1 + \frac{2}{a^2} \right) (c^2 - 4ab) \right]^{1/2}, \quad (22)$$

$$D_{SES} = (c^2 - 4ab)^{1/2}, \quad (23)$$

i.e., DST reduces Euclidean distances between fixed

points by a factor  $(1 + 2/a^2)^{1/2} \simeq 3.7$ .

Also, DST does not preserve the relative orientations of fixed point subspaces. With the aid of symbolic computations, we compute unit eigenvectors spanning the 1D eigenspaces associated with real eigenvalues of the fixed points. The angle between eigenspaces is then found to be  $43.1^\circ$  for the OS, modified by the DST to  $84.9^\circ$  for the SES. Therefore, reduction of Euclidean distances is associated with an increase of the eigenspace relative orientation angle.

We finally comment that DST preserves generalized dimensions  $D_q$  and generalized entropies  $K_q$ . More generally,  $D_q$  and  $K_q$  must be equal for all systems discussed in this paper. (See Sec. V for more extensive discussions.) At this point, we may explain the meaning of equivalent systems in the context of vector-field reconstructions. Our systems are equivalent with respect to the properties that they share. The fact that the  $D_q$  and  $K_q$  are preserved correspond to metric and dynamical equivalences. The whole set of equivalent properties has nevertheless not been up to now systematically identified.

#### E. Reconstruction methods and standard reconstructed systems

Reconstruction methods and SRS's being discussed in Ref. [6], we only here briefly recall some essential information for the sake of completeness. From scalar time series  $\{x_i\}$ , we may determine vectorial time series  $\{x_i, Y_i, Z_i, \dot{Z}_i\}$  by using sufficiently accurate finite-difference scheme. We are then left with the problem of determining the unknown function  $F$ .

This problem may be considered as a problem of multivariate modeling of data, which is rather extensively documented in the literature (see, for instance, Ref. [10]). In Ref. [6], we started by expressing  $F$  as a ratio of polynomial expansions that may be attempted in any case, even when the OS is unknown, a popular choice for forecasting problems [11,12]. We have then to solve a set of linear equations, in which series  $\{x_i, Y_i, Z_i, \dot{Z}_i\}$  provide known coefficients, to be solved against indeterminate elements (reconstructed constants) that are coefficients in the ratio of expansions. Actually, for the sake of accuracy, many sets are solved and averaged results are ob-

TABLE I. Value of reconstructed constants.

Constant	Theoretical value	Reconstructed value	$\epsilon$ (%)
$A$	0.796	0.795 996 958	0.000 38
$B$	-4	-3.999 987 759	0.000 31
$C$	1	1.000 004 939	0.000 49
$E$	1	1.000 005 590	0.000 56
$G$	-3.602	-3.601 987 328	0.000 35
$P$	-0.227 376 080 . . .	-0.277 376 463	0.000 17
$U$	0.137 247 840 . . .	0.137 243 848	0.002 9
$V$	-0.759 982 719 . . .	-0.759 981 069	0.000 22
$W$	0.090 495 680 . . .	0.090 496 341	0.000 73
$S$	0.090 495 680 . . .	0.090 494 834	0.000 93
$T$	-0.227 376 080 . . .	-0.227 374 487	0.000 70

tained. From the results, we may identify a subset of reconstructed constants that must be equal to zero. This identification relies on the following objective grounds: (i) very small absolute values of the corresponding reconstructed constants, (ii) very large standard mean deviations evaluated for each constant on the set of independent evaluations, each of these evaluations being obtained by solving one set of linear equations, (iii) nonreproducibility of the corresponding evaluations when different time series are processed. These two last features indicate that evaluations of the corresponding constants are dominated by numerical noise. After dismissing these constants and rearranging, we then show that  $F$  may be rewritten as

$$\begin{aligned} \dot{Z} = & A + Bx + Cx^2 + ExZ + GZ \\ & + \frac{Y}{1+Px} (U + Vx + Wx^2 + SY + TZ), \end{aligned} \quad (24)$$

in which  $A, \dots, T$  are the nonzero reconstructed constants. Equation (24) defines a standard reconstructed system (SRS) to compare with the SES [Eq. (7)]. Reconstructed constants are again reevaluated by solving new sets of linear equations leading to the results in Table I, in which  $\epsilon$  is the relative difference (in module) between theoretical and reconstructed values. The average  $\epsilon$  per constant is  $7.10^{-4}\%$ .

### III. NUMERICAL STUDY OF STANDARD SYSTEMS

Standard systems are available under the form of SRS's even when the OS and therefore DST and IST are unknown. They play a twofold role. First, they are at the core of the vector-field reconstruction problem by providing an easy way to obtain basic vector fields equivalent to the OS one. They are specified by a set of reconstructed constants. It is of interest to remark that the introduction of these systems addresses the issue of information compression, which might be a significant by-product of our work. Indeed, for a perfect reconstruction, a large amount of original data (the original scalar series) is encoded in a small set of reconstructed constants. Iterating (i.e., integrating) the vector field reproduces a scalar series ideally equivalent to the original one. This is fairly similar in spirit to the case of image encoding, where attracting images are produced by iterated functions systems [13]. Second, SRS's being equivalent to the underlying OS (see the end of Sec. II D and Sec. V), some OS properties may be recovered by studying the SRS's and inverse systems derived from them (Sec. IV).

We now discuss state trajectories. Figure 1 shows a part of a trajectory on the attractor  $A_{SES}$  of the SES. The figure is obtained by integrating the OS and applying the DST to each sampled point. All integrations in this paper are carried out by a fourth-order Runge-Kutta scheme, with a constant step  $\delta t = 10^{-3}$  (except when explicitly stated otherwise) and all figures contain more

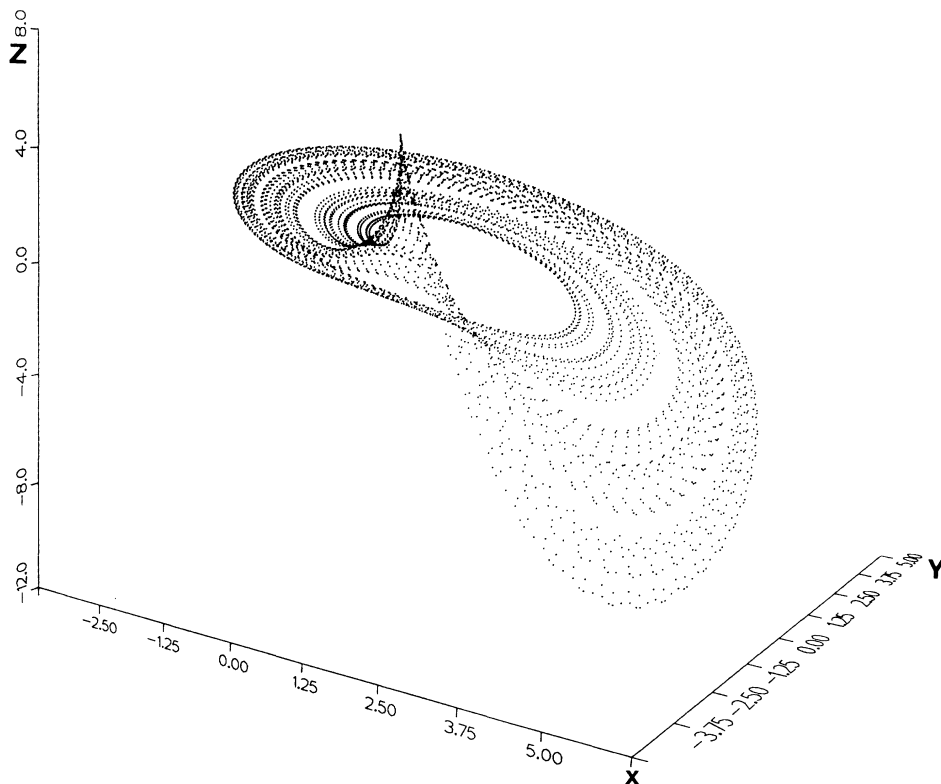


FIG. 1. Attractor of the standard exact system (SES) obtained by applying the direct standard transformation (DST) to the attractor of the original system (OS).

than 5000 sampled points with about 100 sampled points per  $T_0$ . The apparent spike in Fig. 1 is only an artifact resulting from the chosen view angle, and actually corresponds to an upward part of the band, similar to the one going downward in the rightmost part of the figure. We also note that  $x$  regularly becomes bigger than the critical  $x_c = (a + c)$  of the pseudosingular term of the SES equations. However, since there are no singularity problems in integrating the OS or in applying the DST, there was no difficulty in generating a display of  $A_{\text{SES}}$  with the present procedure. We also remark that both fixed points of the SES [Eqs. (20) and (21)] are located inside the band; that is to say, although one fixed point is near the coordinate center and the other is far away from it, both must now be called inner fixed points. This is in contrast with the OS, in which the fixed point near the origin is also an inner point, while the other one is definitely an outer point.

$A_{\text{SES}}$  may also be generated by integrating the SES [Eq. (7)]. However, this procedure is not immediately successful because trajectories may be ejected from the SES and also from its basin of attraction. An example is provided in Fig. 2, in which both kinds of events appear (i.e., ejection from  $A_{\text{SES}}$  followed by reinjection to it, and ejection out of the basin of attraction toward infinity). Nevertheless, the existence of  $A_{\text{SES}}$  is well evidenced by the object looking like a small galaxy in the central part of the figure. Close numerical examination of ejection events shows that they are always associated with the trajectory crossing  $x_c$  although crossing  $x_c$  is safe most of

the time. This is due to the fact that, although the set  $\{x = x_c\}$  is of Lebesgue measure 0, there exists a small numerical unsafe  $x$  domain surrounding the critical  $x_c$ . Preliminary runs demonstrated that the occurrence of ejection events dramatically decreases when the integration time step decreases. This may result from a balance between two contradictory features: (a) a time-step decrease enhances the probability of landing nearer to  $x_c$  but (ii) local truncation errors [8] in a fourth-order Runge-Kutta scheme are proportional to  $(\delta t)^4$ , leading to a decrease of the extension of the unsafe  $x$  domain around  $x_c$ .

The numerical problems associated with  $x_c$  are solved by using a modified integration algorithm relying on the aforementioned observations as follows. Most of the integration is carried out by using a basic time step  $\delta t = 10^{-3}$ . When  $x$  lands in a domain  $(x'_{\min}, x'_{\max})$  surrounding  $x_c$ , the time step is switched to  $\delta t' \ll \delta t$ . We then define an unsafe domain  $(x_{\min}, x_{\max})$  surrounding  $x_c$  but included in  $(x'_{\min}, x'_{\max})$ . When  $x$  lands in the unsafe domain, we compare at each time step the relative difference (in module) between  $\dot{Z}$  computed from the vector-field expression and  $\dot{Z}_{\text{ext}}$  computed by extrapolating from the  $\dot{Z}$  values at the two previous time steps. When this difference is smaller than a preset value  $\epsilon_c$ , the algorithm runs without any intervention. When it is larger than  $\epsilon_c$ ,  $\dot{Z}$  is replaced by the value of  $\dot{Z}$  at the previous time step to evaluate the new  $Z$  value. At each time step when  $\dot{Z}$  and  $\dot{Z}_{\text{ext}}$  are relatively different by more than  $\epsilon_c$ , we say that we have an intervention, i.e.,

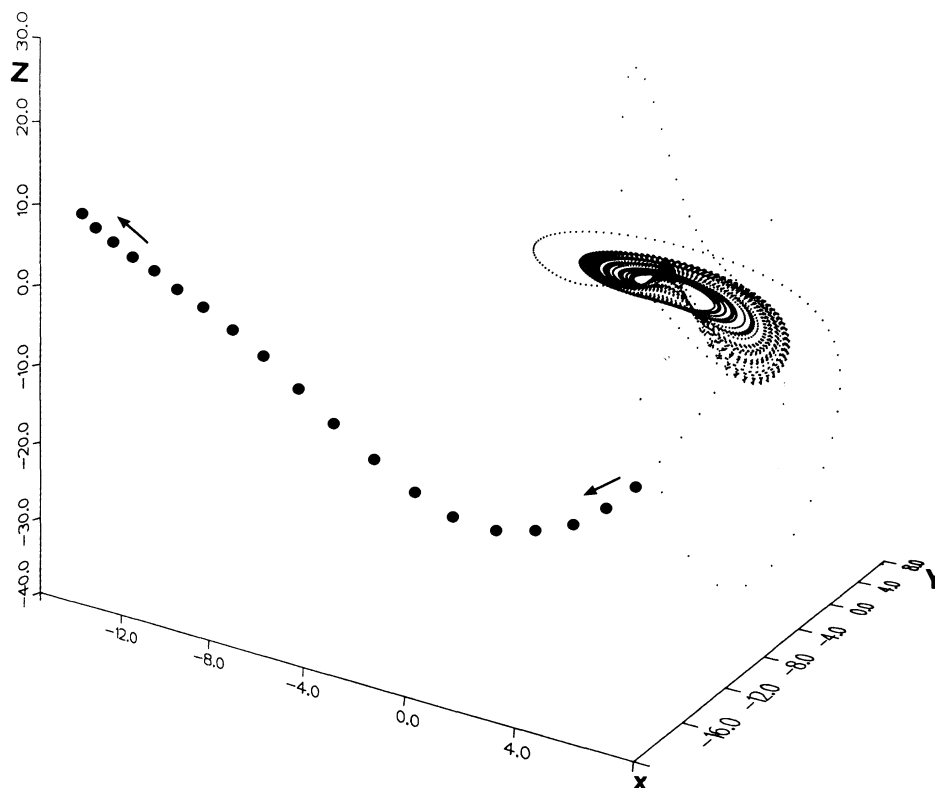


FIG. 2. Examples of ejection events resulting from integrating the SES without any intervention procedure.

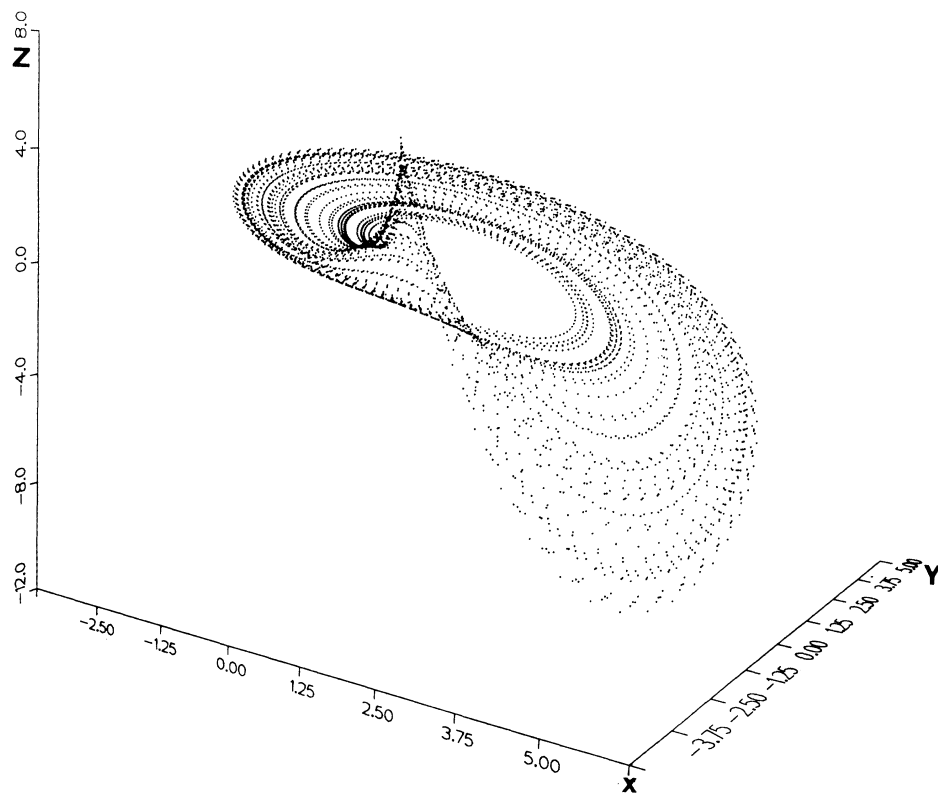


FIG. 3. Attractor of the SES obtained by using an intervention procedure. Compare with Fig. 1.

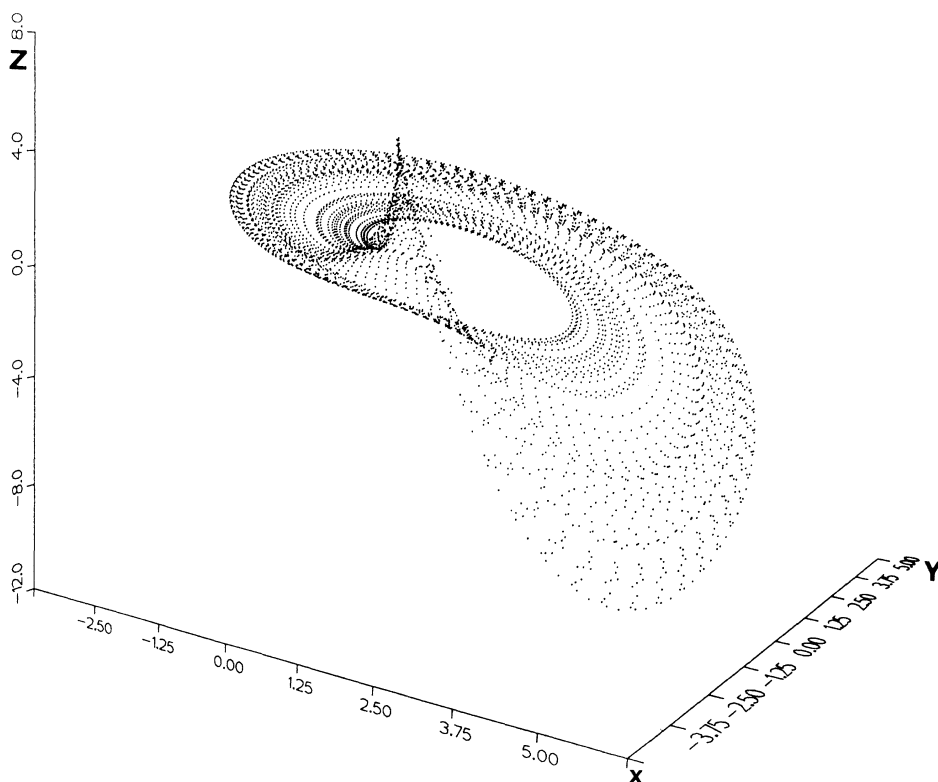


FIG. 4. Attractor of the standard reconstructed system (SRS). Compare with Figs. 1 and 3.

the computed value of  $\dot{Z}$  is replaced by a presumed more accurate one. It usually happens that interventions occur for a number of successive time steps. A set of consecutive interventions is called an accident. For all interventions pertaining to the same accident, the replacement value of  $\dot{Z}$  is kept constant, i.e., it is equal to the replacement value of  $\dot{Z}$  at the first intervention of the accident. The fact that the intervention procedure is implemented for  $x \in (x_{\min}, x_{\max})$  pertaining to a bigger domain  $(x'_{\min}, x'_{\max})$  in which  $\delta t$  is switched to  $\delta t'$  is not strictly necessary but dramatically simplifies the computer program by avoiding the need to account for algorithm edge effects at the frontiers of the unsafe domain. Finally, care is taken to ensure equality of sampling times, although there is no more equality of integration time steps. Figure 3 shows a graphical display of  $A_{\text{SES}}$  obtained by this procedure. The intervention time step  $\delta t'$  was set to  $10^{-7}$  with an unsafe domain (4.395,4.401) included in a  $\delta t$ -switching domain (4.385,4.411) and a tolerance  $\epsilon_c = 2\%$ . For this display corresponding to about  $50T_0$ , the intervention procedure was never activated. Comparison between Figs. 1 and 3 is very satisfactory.

The same modified integration algorithm is used for integrating the SRS [Eq. (24) with Table I reconstructed values]. It is run with  $\delta t' = 5 \times 10^{-8}$ ,  $(x_{\min}, x_{\max})$  and  $(x'_{\min}, x'_{\max})$  unchanged, and a tolerance  $\epsilon_c = 8\%$ . For 5000 units of time, we observed 20 accidents with 55 interventions, i.e., one accident for every  $40T_0$  on average. This is in contrast with the SES, for which no accident was observed on the same running time. We attribute the increase of the number of accidents to the fact that the reconstruction is not perfect. Therefore, the singular term of Eq. (24) is not pseudosingular any more. However, we may state that the amount of parasitic singularity is very small because reconstructed constants are obtained with a high accuracy. Note that  $\delta t'$  and  $\epsilon_c$  were modified with respect to the SES case. Although the number of accidents tends to decrease when  $\delta t'$  decreases, there is a need to compromise between accuracy and CPU requirements. There is also a need to compromise with  $\epsilon_c$  because  $\epsilon_c$  too small leads to too many interventions, some of them being possibly undue.

Figure 4 shows a graphical display of  $A_{\text{SRS}}$  for again about  $50T_0$ , which compared very favorably with the  $A_{\text{SES}}$  in Fig. 3. Discussions of quantitative validations are postponed to Sec. V.

#### IV. INVERSE SYSTEMS

When OS's are unknown, SRS's form the basic vector fields equivalent to the OS's. We may afterward generate an infinite number of other equivalent systems, called inverse systems, obtained by using inverse transformations taking standard coordinates  $(x, Y, Z)$  to new coordinates  $(x', y', z')$ . For experimental systems, one interesting question is to know whether inverse coordinates  $(x', y', z')$  may be chosen such that they would have a clear physical meaning. In this paper, we only consider a subclass of inverse systems such as  $x \equiv x'$ . Furthermore, there exists special inverse systems of particular interest when the OS's are known, as is discussed below.

##### A. Inverse standard systems

When the OS and therefore the DST [Eqs. (8)–(10)] are known, we may use an inverse standard transformation (IST), taking standard coordinates  $(x, Y, Z)$  back to the original ones  $(x, y, z)$ , producing inverse standard systems (ISS's). In this paper, ISS's are defined by using the DST and demanding that the two last equations for  $\dot{y}$  and  $\dot{z}$  of the OS [Eqs. (2)–(3)] be exactly satisfied. Therefore, all numerical errors associated with reconstructions are reported on the first equation for  $\dot{x}$ . For a given reconstruction, IST then produces an inverse standard reconstructed system (ISRS) taking the form

$$\dot{x} = F'(x, y, z), \quad (25)$$

$$\dot{y} = x + ay, \quad (26)$$

$$\dot{z} = b + z(x - c). \quad (27)$$

For the SRS of Eq. (24), we then find that the ISRS is given by

$$\dot{x} = \frac{-1}{1+z} \left[ (A - Gb - bc) + x(B + a + b - Eb - g) + ya(a - G) + zc(G + c) + x^2(C - E) - xyaE \right. \\ \left. + xz(Ec - G - 2c) + x^2z(1 - E) + \frac{y+z}{1+Px} [(bT - U) + x(T - V) + y(S + aT) + z(S - cT) - x^2W + xzT] \right]. \quad (28)$$

Again a set of singularities of Lebesgue measure 0 appears in (28). However, giving the constants  $A, \dots, T$  their exact theoretical values, we define an inverse standard exact system (ISES), which simply identifies with the

OS with no singularity and even no pseudosingularity. Therefore, for a high-quality reconstruction, the amount of singularity is very small. As a consequence, it has been possible to integrate the ISRS without any intervention

procedure. OS and ISRS graphical displays are shown in Figs. 5 and 6, respectively, comparing very favorably. Quantitative validations are postponed to Sec. V.

### B. Inverse nonstandard systems

The interest of using ISS when the OS is known is to provide the reader with immediate and direct convincing validations of the reconstruction because comparisons are achieved against the OS itself. However, when the OS is unknown, we can only discuss inverse nonstandard systems (INSS) in which phase coordinates are  $(x', y', z') \neq (x, y, z)$ . Variable  $x$  being the one of the original scalar series, we may, however, choose  $x \equiv x'$ . The number of INSS being infinite, choices must be motivated. Motivation may come from the fact that there are some disadvantages in using standard systems due to the existence of pseudosingular terms in SES and of parasitic singular terms in SRS requiring the use of an intervention procedure to integrate the systems. We then decide to examine INSS in which such terms would disappear or at least would be small enough to avoid the need for the intervention procedure.

As a first example, we examine an exact case, starting from the SES [Eq. (7)] to produce an inverse nonstandard exact system (INSES). We set

$$\gamma = \frac{x + b - aY + Z}{k(a + c - x)}, \quad (29)$$

in which  $k$  is a free constant in such a way that Eq. (7) for  $\dot{Z}$  may be rewritten

$$\begin{aligned} \dot{Z} = & ab - cx + x^2 - axY + xZ + (ac - 1)Y \\ & + (a - c)Z - kY\gamma. \end{aligned} \quad (30)$$

Expressing  $Z$  from (29) and deriving, we obtain a second expression for  $\dot{Z}$  (using also  $\dot{x} = Y, \dot{Y} = Z$ ) which is identified with (30). With the aid of (29) again, we find

$$\dot{\gamma} = \frac{b}{k} + \gamma(x - c), \quad (31)$$

in which no pseudosingular term appears.

We shall produce an INSES with coordinates  $(x, \beta, \gamma)$ . For  $\dot{x}$ , we are free to choose

$$\dot{x} = k_x x + k_\beta \beta + k_\gamma \gamma, \quad (32)$$

defining a class of inverse systems in which the first equation is chosen to be linear for the sake of simplicity

The equation for  $\dot{\beta}$  is afterward obtained by using (32) derived with respect to time and manipulating the resulting expression to produce

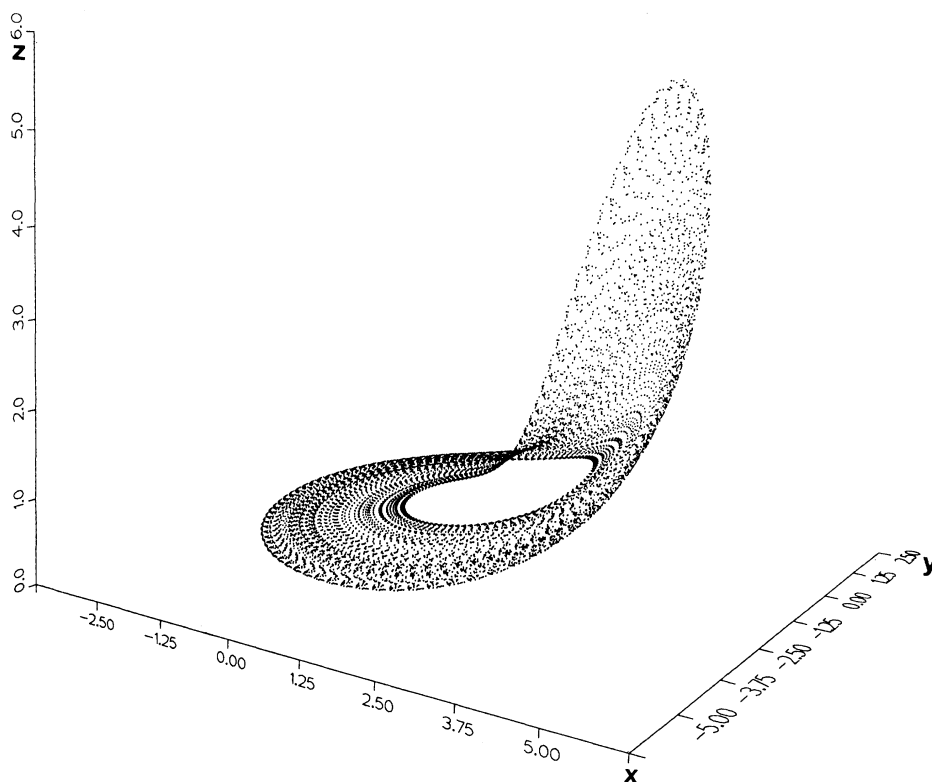


FIG. 5. Attractor of the original system (OS).

$$\dot{\beta} = \frac{1}{k_\beta} \left[ -b \left[ 1 + \frac{k_\gamma}{k} \right] + x(ak_x - 1 - k_x^2) + \beta k_\beta(a - k_x) + \gamma[(a + c)(k + k_\gamma) - k_x k_\gamma] - \gamma x(k + k_\gamma) \right]. \tag{33}$$

We have therefore obtained a class of inverse systems with free constants  $(k, k_x, k_\beta, k_\gamma)$  without any singularity. For the sake of simplicity, it is advantageous to choose  $k_\gamma = -k$ , removing the nonlinear term in (33). If we also take  $k_x = k_\beta = k_\gamma = 1$ , we obtain the INSES:

$$\dot{x} = x + \beta + \gamma, \tag{34}$$

$$\dot{\beta} = (a - 2)x + (a - 1)\beta - \gamma, \tag{35}$$

$$\dot{\gamma} = -b + \gamma(x - c). \tag{36}$$

Also, with  $k_x = 0, k_\beta = k_\gamma = -1$ , we obtain another INSES which identifies with the OS.

Similarly, we now start from the SRS [Eq. (24)] to produce a class of inverse nonstandard reconstructed systems (INSRS's). In a first step, we remove all nonlinear terms in the singular term of Eq. (24) leading to

$$\dot{Z} = A + Bx + Cx^2 + \frac{W}{P}xY + ExZ + \mathcal{F}Y + GZ + \frac{Y}{1 + Px} \left[ (U - \mathcal{F}) + \left[ V - \mathcal{F}P - \frac{W}{P} \right] x + SY + TZ \right], \tag{37}$$

in which a free constant  $\mathcal{F}$  had to be introduced. Then we set

$$\phi = \frac{(U - \mathcal{F}) + (V - \mathcal{F}P - W/P)x + SY + TZ}{K(1 + Px)}, \tag{38}$$

$$\dot{x} = K_x x + K_\psi \psi + K_\phi \phi, \tag{39}$$

and proceeds similarly as before to obtain

$$\dot{\psi} = \dot{\psi}(x, \psi, \phi), \tag{40}$$

$$\dot{\phi} = \dot{\phi}(x, \psi, \phi), \tag{41}$$

depending on free constants  $\mathcal{F}, K, K_x, K_\psi, K_\phi$ . Relations (40) and (41) are too lengthy to be given here and were actually obtained with the aid of symbolic computations. We then afterward choose  $\mathcal{F} = 0, K = K_x = K_\psi = K_\phi = 1$  and obtain the following INSRS:

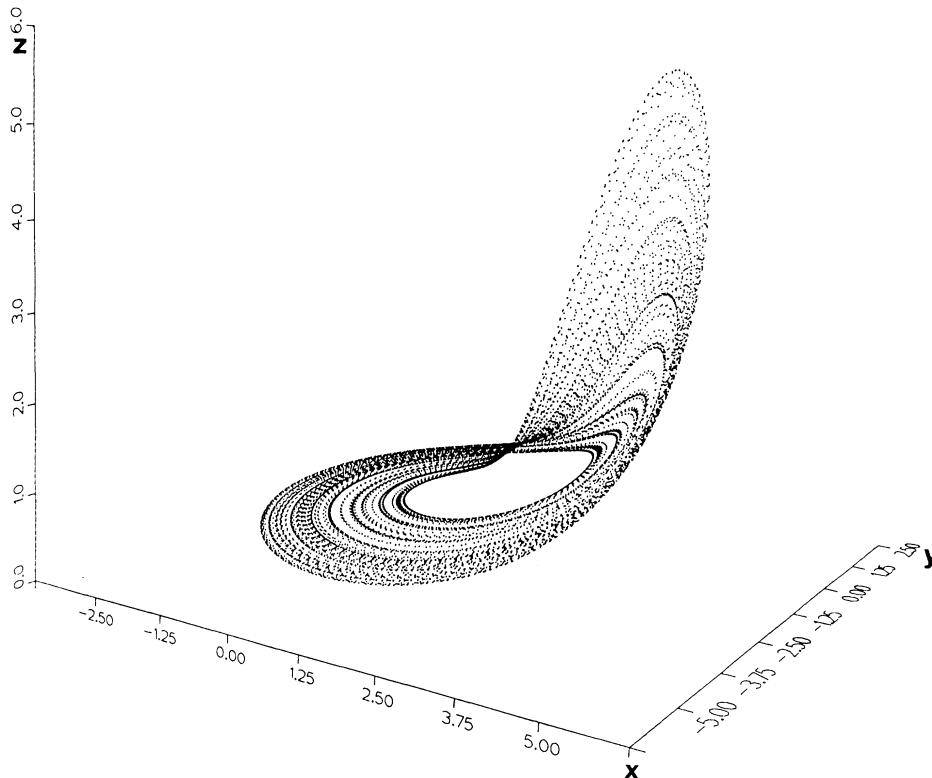


FIG. 6. Attractor of the inverse standard reconstructed system (ISRS). Compare with Fig. 5.

$$\dot{x} = x + \psi + \phi, \tag{42}$$

$$\begin{aligned} \dot{\psi} = & \left[ -\frac{U}{T} - \left( 1 + \frac{S}{T} \right) (x + \psi) + \frac{1}{T} \left( \frac{W}{P} - V \right) x + \left( \frac{1}{T} - 2\frac{S}{T} - G \right) \phi + \left( \frac{P}{T} - E \right) x\phi \right] \\ & + \frac{1}{1+Px} \left\{ \left[ \frac{SU}{T} - AT + GU \right] + \left[ \frac{W}{P} + \frac{S^2}{T} + GS - V + \left[ ES - \frac{WT}{P} \right] x \right] (x + \psi + \phi) \right. \\ & \left. + \left[ EU + GV - BT + \frac{SV}{T} - \frac{GW}{P} - \frac{SW}{PT} \right] x - \phi + \left[ EV - CT - \frac{EW}{P} \right] x^2 - Tx\phi + (P - T)\phi(\phi + \psi) \right\}, \end{aligned}$$

$$\dot{\phi} = \left[ G + \frac{S}{T} + Ex \right] \phi + \frac{1}{1+Px} \left\{ \left[ AT - GU - \frac{SU}{T} \right] \left[ V - GS - \frac{W}{P} - \frac{S^2}{T} + \left[ \frac{TW}{P} - ES \right] x + (T - P)\phi \right] \right. \tag{43}$$

$$\left. \times (x + \psi + \phi) + \left[ BT - EU - GV + \frac{GW}{P} - \frac{SV}{T} + \frac{SW}{TP} \right] x + \left[ CT - EV + \frac{EW}{P} \right] x^2 \right\}. \tag{44}$$

Singular terms in (43) and (44) reduce to 0 as expected when reconstructed constants  $A, \dots, T$  are given their exact theoretical values. In the actual INSRS, they are again very small due to the quality of the reconstruction, with the consequence that no intervention procedure is required to integrate the system. Therefore our aim is fulfilled.

The INSES obtained by injecting the theoretical values of the reconstructed constants in the INSRS reads

$$\dot{x} = x + \psi + \phi, \tag{45}$$

$$\dot{\psi} = a(ac - 1) + (a - 2)x + (a - 1)\psi - \phi, \tag{46}$$

$$\dot{\phi} = -b + (\phi + 1 - ac)(x - c). \tag{47}$$

Coordinates  $(x, \psi, \phi)$  of this INSES and  $(x, y, z)$  of the OS are related by a nonsingular everywhere-invertible transformation

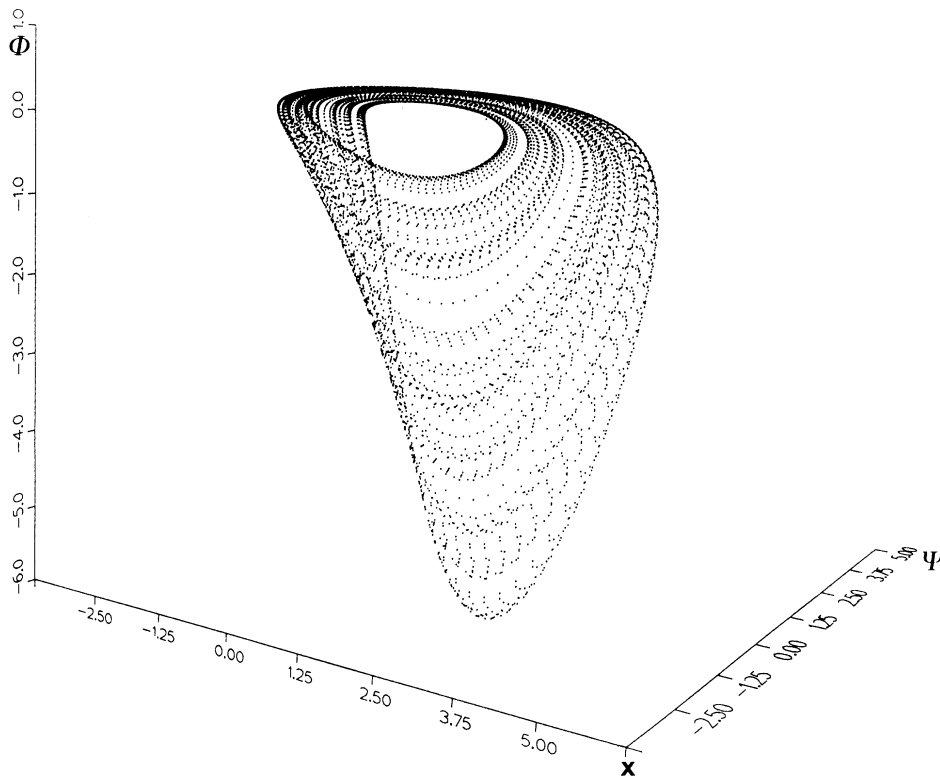


FIG. 7. Attractor of the inverse nonstandard exact system (INSES).

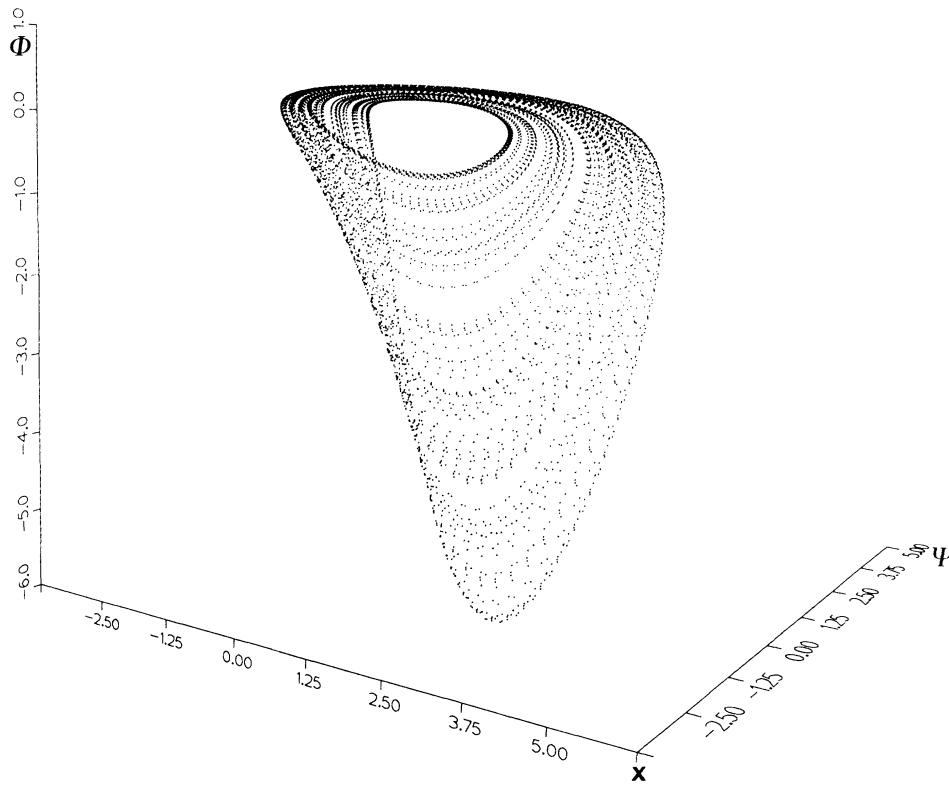


FIG. 8. Attractor of the inverse nonstandard reconstructed system (INSRS). Compare with Fig. 7.

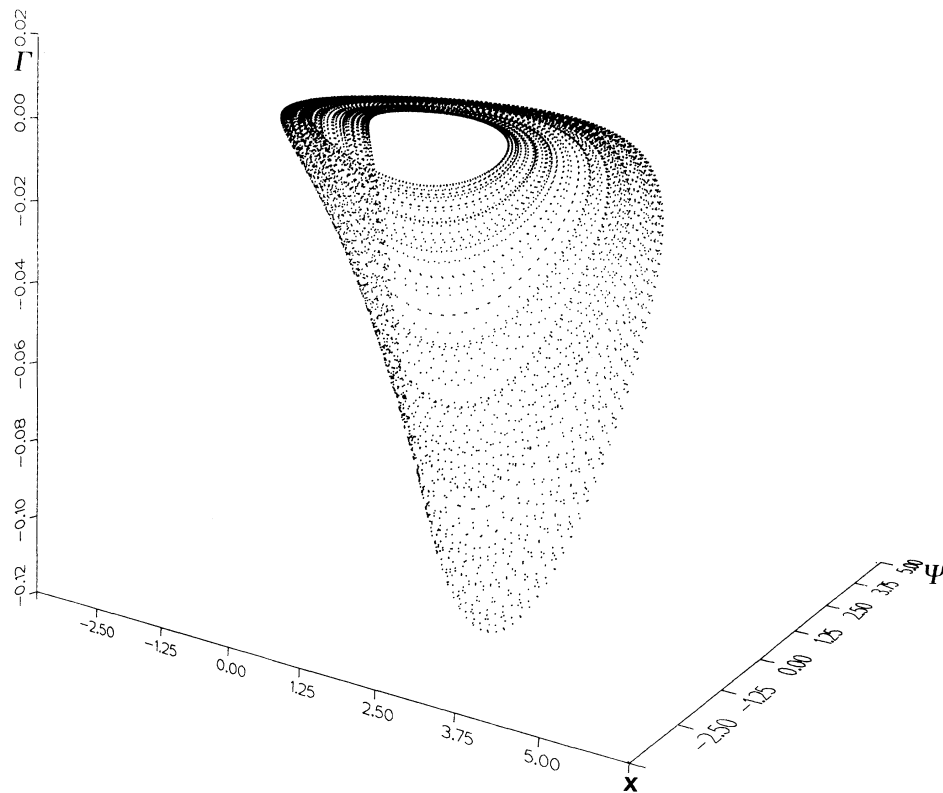


FIG. 9. Attractor of the squeezed inverse nonstandard exact system (SINSES). Compare with Fig. 7.

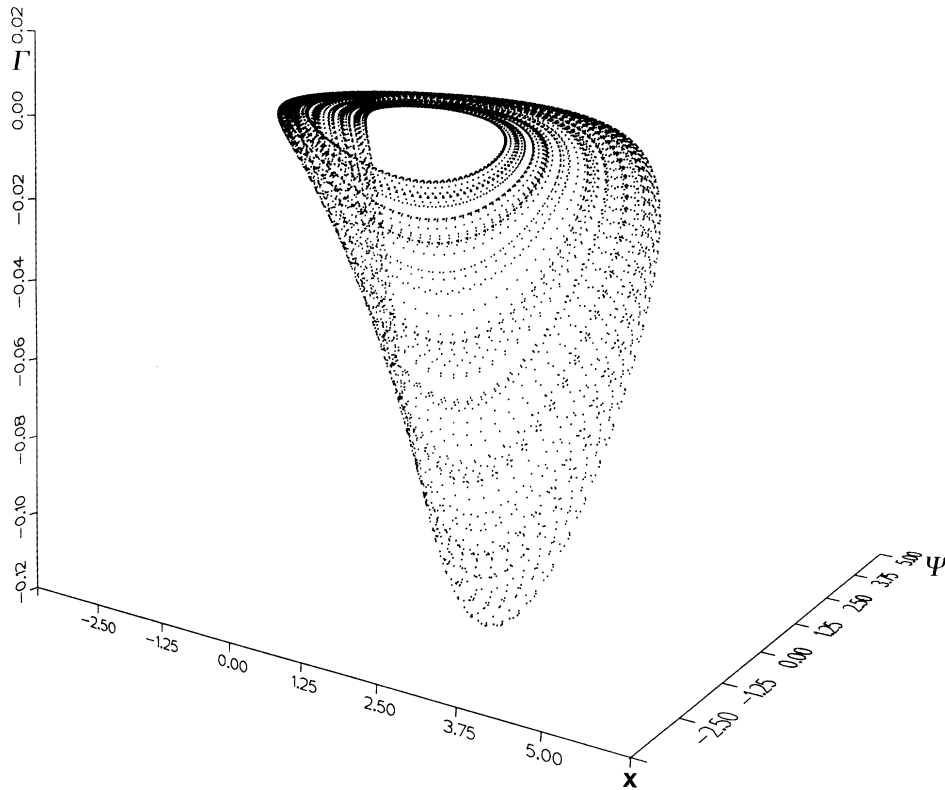


FIG. 10. Attractor of the squeezed inverse nonstandard reconstructed system (SINSRS). Compare with Fig. 9.

$$\begin{aligned}
 x &= x, \\
 \psi &= 1 - ac - (x + y), \\
 \phi &= ac - 1 - z; \\
 x &= x, \\
 y &= 1 - ac - (x + \psi), \\
 z &= ac - 1 - \phi,
 \end{aligned}
 \tag{48}$$

$$\begin{aligned}
 x &= x, \\
 y &= 1 - ac - (x + \psi), \\
 z &= ac - 1 - \phi,
 \end{aligned}
 \tag{49}$$

in which we should note the perfect correspondence between direct and inverse transformations. The other INSES introduced previously [Eqs. (34)–(36)] may be similarly recovered from the class (39)–(41) by specifying again  $K = K_x = K_\psi = K_\phi = 1$  but  $\mathcal{F} = (ac - 1)$ .

Graphical displays of an INSES [Eqs. (45)–(47)] and of the corresponding INSRS [Eqs. (42)–(44)] are given in Figs. 7 and 8, respectively, evidencing the quality of the reconstruction. Again, quantitative validations concerning generalized dimensions are postponed to Sec. V. We shall, however, remark that evaluations of  $D_q$ 's for  $q$  smaller than typically 1 are impossible for the INSRS. We shall also comment that this difficulty might be solved by considering new inverse systems in which the third coordinate  $\phi$  would be squeezed by a large factor according to

$$\Gamma = \phi / 50. \tag{50}$$

Introducing Eq. (50) in INSES and INSRS, we obtain a

squeezed INSES (SINSES) and a squeezed INSRS (SINSRS), respectively, with coordinates  $(x, \psi, \Gamma)$ . Graphical displays of SINSES and SINSRS are shown in Figs. 9 and 10, respectively, looking very much like Figs. 7 and 8, as expected. Note, however, the modification of the vertical scale induced by Eq. (50).

## V. GENERALIZED DIMENSIONS

Quantitative validations rely on the comparison between generalized dimensions of the various systems discussed in the previous sections. For convenience, the identification of these systems is summarized below.

- (1) Original system (OS), with coordinates  $(x, y, z)$ . See Eqs. (1)–(3) and Fig. 5.
- (2) Inverse standard reconstructed system (ISRS), with coordinates  $(x, y, z)$ . See Eqs. (25)–(28) and Fig. 6.
- (3) Standard exact system (SES), with coordinates  $(x, Y, Z)$ . See Eqs. (4)–(7) and Figs. 1 and 3.
- (4) Standard reconstructed system (SRS), with coordinates  $(x, Y, Z)$ . See Eqs. (4)–(6) and (24), and Fig. 4.
- (5) Inverse nonstandard exact system (INSES), with coordinates  $(x, \psi, \phi)$ . See Eqs. (45)–(47) and Fig. 7.
- (6) Inverse nonstandard reconstructed system (INSRS), with coordinates  $(x, \psi, \phi)$ . See Eqs. (42)–(44) and Fig. 8.
- (7) Squeezed inverse nonstandard exact system (SINSES), with coordinates  $(x, \psi, \Gamma)$ . See Eqs. (45)–(47) and (50), and Fig. 9.
- (8) Squeezed inverse nonstandard reconstructed system

(SINSRS), with coordinates  $(x, \psi, \Gamma)$ . See Eqs. (42)–(44) and (50) and Fig. 10.

In any case, generalized dimensions are computed by a fixed-radius algorithm of the Grassberger-Procaccia kind in the phase space of the considered system ( $\mathbb{R}^3$ ), i.e., without any reconstruction of the attractor in  $\mathbb{R}^n$ . Formulations and more precise definitions of the algorithms we used are available from Refs. [6] and [9], in which an extensive pioneering literature is also quoted. About 60 vectors are sampled per pseudoperiod  $T_0$ . The resolution  $(N, m)$  is  $(10^6, 2000)$  in which  $N$  is the total number of sampled points and  $m$  is the number of central vectors used to average local correlation moments. Local slopes  $D_q(r_i)$  are evaluated at 45  $r_i$  locations separated by equal logarithmic intervals on a range  $(r_1, r_2)$ . The  $D_q$  are afterward obtained by averaging local slopes in a  $r$ -scaling domain  $(r_{\min}, r_{\max})$ . We obtain an insight on the accuracy of the results from the standard mean deviation  $\sigma_D$  of the local-slope values in the  $r$ -scaling domain. It is well known that the choice of the  $r$ -scaling domain lacks objectivity in this algorithm and that this feature is actually one of its shortcomings. Furthermore, the range  $(r_{\min}, r_{\max})$  depends on  $q$ . Therefore, we should ideally present specific data to express  $r_{\min}(q), r_{\max}(q)$ . However, to avoid data proliferation, we shall only mention that our results are rather insensitive to reasonable modifications of the  $r$ -scaling domain. Also, instead of being interested in exact values of  $D_q$  we are more concerned with comparisons between  $D_q$  values. Good comparisons provide reconstruction validations, even if the  $D_q$  values themselves are biased. Therefore, exact and reconstructed systems of the same kind (for instance, SES and SRS, or INSES and INSRS) are studied with the same ranges  $(r_{\min}, r_{\max})$  in such a way that comparisons make sense, except for one case to be mentioned later. Some of our results are summarized in Table II for a significant choice of values of  $q$ 's ranging from  $[-50$  to

$+50]$ . We note that  $D_q$ 's become smaller than 2 when  $q$  is big enough, a result that we do not believe to be correct for hyperbolic strange attractors (see complementary discussions on this point in Refs. [6] and [9]). However, again, comparisons make sense because computer programs for exact and corresponding reconstructed systems have been run under the same specifications.

We now come to a detailed discussion of these results. One question to be answered is, what are acceptable differences between  $D_q$  values. We might rely on  $\sigma_D$  and state that it provides an error in the data. Comparisons between  $D_q$  values of the various studied systems ( $q$  fixed) would then be satisfactory if the dimensions did not spread too much outside of the error. However,  $\sigma_D$  provides a very poor and actually unreliable estimation of the inaccuracies produced by the computations. For instance, using data for the OS, we would be amenable to accepting  $D_{-50} = 2.28 \pm 0.15$  and  $D_{+50} = 1.63 \pm 0.23$  according to  $D_q$  values presented in Table II and corresponding values we obtained for  $\sigma_D$ 's. If we except columns (7) and (8) for the squeezed systems, which deserve special discussion, it is clear than the obtained results are in better agreement than what  $\sigma_D$  would tell us to accept. Therefore, being satisfied with data interpretation relying on  $\sigma_D$  might lead to optimistic statements. Another more severe and consequently better way to proceed is to derive standard mean deviations  $\sigma'_D$  obtained by making statistics on exact system columns (1,3,5,7). Although poorly evaluated,  $\sigma'_D$  would provide us with a more realistic criterion to examine  $D_q$  comparisons. However, this discussion only makes sense if we previously answer a second question: are  $D_q$  values invariant under coordinate changes?

This question is discussed by Ott, Withers, and Yorke [14]. The authors emphasize that, to be proper dimensions, quantities should be invariant under a reasonable change of coordinates. Then they show that the  $D_q$ ,

TABLE II. Comparison between generalized dimensions  $D_q$ . Columns (1)–(8) concern the original system (OS), the inverse standard reconstructed system (ISRS), the standard exact system (SES), the standard reconstructed system (SRS), the inverse nonstandard exact system (INSES), the inverse nonstandard reconstructed system (INSRS), the squeezed inverse nonstandard exact system (SINSES), and the squeezed inverse nonstandard reconstructed system (SINSRS), respectively.

$q$	(1)	(2)	(3)	(4)	(5)	(6)	(7)	(8)
-50	2.28	2.32	2.14	2.15	2.18		2.23	2.44
-40	2.27	2.31	2.13	2.15	2.17		2.23	2.44
-30	2.26	2.31	2.13	2.14	2.17		2.23	2.43
-20	2.24	2.29	2.12	2.12	2.16		2.22	2.41
-10	2.18	2.23	2.10	2.07	2.20		2.19	2.35
-5	2.13	2.21	2.00	2.04	2.15		2.13	2.24
-1	2.00	2.03	1.98	2.03	2.00		2.04	2.07
0	1.960	1.987	1.966	2.060	1.966		1.989	2.004
1	1.917	1.949	1.929	1.944	1.929	1.928	1.933	1.948
2	1.880	1.915	1.899	1.899	1.893	1.885	1.866	1.884
5	1.796	1.836	1.847	1.834	1.804	1.787	1.680	1.662
10	1.707	1.749	1.779	1.768	1.734	1.710	1.512	1.480
20	1.654	1.681	1.733	1.729	1.664	1.641	1.403	1.377
30	1.641	1.659	1.719	1.717	1.647	1.625	1.360	1.348
40	1.635	1.650	1.713	1.712	1.637	1.617	1.338	1.336
50	1.630	1.645	1.709	1.708	1.631	1.611	1.326	1.330

$q \neq 1$ , fail this test. They therefore should not be called dimensions. However, under a reasonable change of coordinates, the information dimension  $D_1$  (and also the Hausdorff dimension, not discussed in this paper) is invariant. Consequently, we first concentrate on this quantity. Considering all the exact systems (columns 1,3,5,7 in Table II), we admit that the spreading between data reflects the uncertainty of our evaluations and then estimate  $D_1 = 1.93 \pm 0.01$ . If we also admit that  $\sigma'_D$  for reconstructed systems would have the same value 0.01, we must be very satisfied when comparison between  $D_1 = 1.93$  and  $D_1$  for a reconstructed system is better than a relative difference  $\epsilon_s \%$ , here found equal to be 1%. In Table III, we display the actual relative differences  $\epsilon_i \%$  observed for the reconstructed systems in columns  $i=2, 4, 6$ , and 8. We conclude that our quantitative validation of the quality of our vector-field reconstruction, relying on  $D_1$ , is therefore very satisfactory.

Although the  $D_q$ ,  $q \neq 1$ , are not invariant according to Ott, Withers, and Yorke, we now heuristically show that all the changes of coordinates considered in this paper are special enough to ensure invariance. We first consider exact systems. They use coordinates  $(x, y, z)$ ,  $(x, Y, Z)$ ,  $(x, \psi, \phi)$ , and  $(x, \psi, \Gamma)$ . In each case, dimensions  $D_q$  have been evaluated by running the algorithms in the corresponding  $\mathbb{R}^3$  phase space. However, according to Takens's theorem, the same information might have been obtained by working in  $\mathbb{R}^n$  and reconstructing attractors from a single variable such as  $x$ . Since variable  $x$  is shared by all exact system, we conclude that  $D_q$  should be invariant. The argument extends to reconstructed systems for perfect reconstructions. Consequently, comparisons between  $D_q$  do provide a test for the quality of the reconstruction. Generalized dimensions  $K_q$ 's would be similarly shown to be invariant.

The fixed-radius algorithm is more efficient for  $q > 1$  than for  $q < 1$ . This is due to the fact that the  $D_q$ ,  $q$  large,

probe the parts of the attractor where the measure is the most concentrated (and conversely for small  $q$ 's). Therefore, statistics become poor in balls of fixed radius when  $q$  becomes small leading to inaccurate  $D_q$  evaluations. The pivot value is shown to be  $q = 1$ . For  $q < 1$ , a fixed mass algorithm might be recommended. Accordingly, we separately discuss the two cases.

For  $q > 1$ , squeezed systems are not considered. For these systems, Table II (columns 7 and 8) clearly shows that the  $D_q$  are strongly underestimated, a fact to be explained later. Similarly as for  $D_1$ , we evaluate  $D_q \pm \sigma'_D$  on the other exact systems (columns 1, 3, and 5) and report values of  $\epsilon_s$  and  $\epsilon_i$  in Table III, except again for the squeezed system. Our quality criterion being satisfied in all cases, we conclude that our results are very satisfactory. The dimension  $D_2$  (the correlation dimension) deserves a special mention because it is of widespread use and its evaluation is reputed to be the easiest and most accurate, as confirmed by the  $\epsilon_s$  value.

We proceed similarly for  $q < 1$ , including now the squeezed systems. We remark (column 6) that evaluations of the  $D_q$ ,  $q < 1$ , have been impossible for the INSRS, indicating enhanced numerical difficulties for these  $D_q$ , as expected. Also, modifications of the  $r$ -scaling domain of the SRS (column 4) were required with respect to the SES for these  $q$ 's. Besides enhanced difficulties when evaluating these  $D_q$  with a fixed-radius algorithm, this fact might also indicate some modifications of the parts of the attractor where the measure is most rarefied because of the increase in the number of interventions required to integrate the SRS when compared to the SES (Sec. III). Proceeding again similarly as for  $D_1$ , we obtain the results displayed in Table III, which are again very satisfactory for columns 2 and 4. For  $q \leq -10$  and column 8, the quality criterion is not strictly satisfied, but, owing to difficulties in evaluating these  $D_q$ , we may conclude that results are satisfactory

TABLE III.  $D_q$  comparisons to validate the quality of reconstructions. Columns (2), (4), (6), and (8) concern reconstructed systems with the same column labels as in Table II.

$q$	$D_q \pm \sigma'_D$	$\epsilon_s$ (%)	(2)	(4)	(6)	(8)
-50	$2.21 \pm 0.06$	6	5	3		11
-40	$2.20 \pm 0.06$	6	5	2		11
-30	$2.20 \pm 0.06$	5	5	3		11
-20	$2.18 \pm 0.06$	5	5	3		10
-10	$2.17 \pm 0.05$	4	3	4		8
-5	$2.07 \pm 0.09$	9	7	1		8
-1	$2.00 \pm 0.03$	3	1	1		3
0	$1.97 \pm 0.01$	1	0.9	5		2
1	$1.93 \pm 0.01$	1	1	0.9	0.05	1
2	$1.89 \pm 0.01$	1	1	0.5	0.2	
5	$1.82 \pm 0.03$	3	1	1	2	
10	$1.74 \pm 0.04$	5	0.5	2	2	
20	$1.69 \pm 0.06$	7	0.7	2	3	
30	$1.67 \pm 0.05$	6	0.6	3	3	
40	$1.66 \pm 0.05$	6	0.7	3	3	
50	$1.66 \pm 0.05$	6	1	3	3	

enough. Again, we should give special mention to  $D_0$ , which has special meaning, i.e., it is the capacity of the support of the measure on the attractor.

We now specifically comment on squeezed systems and the reason why we introduced them. We note in Tables II and III that we have been able to evaluate the  $D_q$ ,  $q < 1$ , for the INSES (column 5) but have been unable to do so for the INSRS. In view of the favorable comparison between Figs. 7 and 8, this might be at first surprising. However, we remember that the discussed  $D_q$  probe parts of the attractor where the measure is the most rarefied, leading to poor statistics. Therefore, even small modifications of the attractor in the reconstruction process might have dramatic consequences for these parts by enhancing the poor statistics problem. It does not necessarily mean that the reconstruction is poor, but that, for these evaluations, we could be on the statistical frontier between what is feasible and what is unfeasible. As a matter of fact, it probably could have been possible that  $D_q$  computations were feasible for the INSRS and not for the INSES, this being essentially an insignificant matter of chance. Examining Figs. 7 and 8, it looks like the relevant rarefied parts are located in the downward lump below the horizontal part of the band. Whether or not this discussion is correct in all respects, it suggests that one might squeeze the vertical coordinate by using Eq. (50) to increase the density of the rarefied parts and produce improved statistics. Indeed, we then find that the  $D_q$ ,  $q < 1$ , are satisfactorily evaluated for both exact and reconstructed squeezed systems (columns 7 and 8).

There is, however, a penalty for that, namely severe underestimations of the  $D_q$ ,  $q > 1$ , well evidenced in Table II. The reason may be explained as follows. These  $D_q$  probe parts of the attractor where the measure is the most concentrated. These parts are seemingly located in the horizontal part of the band, which must also, however, have a certain typical thickness. By squeezing the system, this thickness is also squeezed, without, however, squeezing the horizontal extensions of the attractor. Therefore, an adequate spatial resolution of the fractal would require an examination at smaller distances  $r$ , requiring an increase of the number of sampled points, which might be impossible due to computational resources. A complementary and fairly similar discussion of the problem of  $D_q$  underestimations in band structures may be found in Ref. [9] in the case of a strange attractor produced by a model of thermal lens oscillations. We were consequently motivated on objective grounds in rejecting  $D_q$  data ( $q > 1$ ) for the squeezed systems.

Usually, for measuring the  $D_q$ ,  $q < 1$ , a fixed-mass, instead of a fixed-radius, approach is recommended. This could have been carried out in the case of the INSRS, for which evaluation of these  $D_q$  was not feasible, but was not necessary for the other systems. For the INSRS,

evaluations became feasible when introducing a coordinate squeezing. More generally, we may forecast that coordinate changes could help in evaluating attractor invariants, in mathematical models as well as in experimental systems, providing us with a new alternative to gain accuracy. Although this line of research is outside of our present motivations, it might be worthwhile to devote more time to it. However, we stress that our discussion of squeezed systems has essentially been heuristic and somewhat intuitive. Our last suggestions are therefore only a by-product, which might later turn out not to be productive.

## VI. CONCLUSION

We emphasized that the knowledge of numerical scalar time series permits the reconstruction of vector fields equivalent to the underlying vector field. Reconstruction methods and extensive discussions of several kinds of equivalent systems have been provided. Although we examined the special case of the Rössler band, we indicated how generalizations could be possible to investigate more complicated cases, and therefore established a general framework that should be rather robust with respect to future developments. Here, the word robust means that, although we may later need to generalize the way to determine the standard function  $F$  for more complicated vector fields, or to solve a noise smoothing and/or noise removal problem for studying noisy data, most of the structure of our work is expected to be preserved. See Ref. [3] for the Lorenz system, showing that nothing essential had to be modified to investigate this case. We are currently working on a still more complicated vector field produced by a model of thermal lens oscillations [9] which will require more sophisticated approaches to approximate the standard function  $F$ . Simultaneously, we are investigating the issue of noise smoothing and noise removal. Also, quantitative validations may rely not only on generalized dimensions (or generalized entropies) but also on all the quantities that are preserved by the introduced transformations. A complete list of such quantities, still to be established, would fully define the concept of equivalence used in this paper. Although many lines of research are opened by the present work and many questions still remain to be answered, the most interesting prospect in our opinion might be the possibility of automatic reconstruction of phenomenological models of experimental systems. It would then provide the applied scientist with a new tool of utmost interest.

## ACKNOWLEDGMENTS

The Laboratoire d'Énergétique des Systèmes et Procédés is a part of "Unité Associée au Centre National de la Recherche Scientifique No. 230."

[1] F. Takens, in *Dynamical Systems and Turbulence*, edited by D. A. Rand and L. S. Young, Lecture Notes in Mathematics Vol. 898 (Springer-Verlag, Berlin, 1981) pp. 366–381.

[2] F. Takens, in *Nonlinear Dynamics and Turbulence*, edited by G. I. Barenblatt, G. Iooss, and D. D. Joseph (Pitman, New York, 1983), pp. 314–332.

[3] G. Gouesbet, *Automatic Reconstruction of Dynamical Sys-*

- tem Equations from Numerical Scalar Time Series*, Proceedings of the Eighth Symposium on Turbulent Shear Flows (Technical University of München, München, 1991).
- [4] N. H. Packard, J. P. Crutchfield, J. D. Farmer, and R. S. Shaw, *Phys. Rev. Lett.* **45**, 712 (1980).
- [5] J. Cremers and A. Hübler, *Z. Naturforsch. Teil A* **42**, 797 (1987).
- [6] G. Gouesbet, *Phys. Rev. A* **43**, 5321 (1991).
- [7] J. M. T. Thompson and H. B. Stewart, *Nonlinear Dynamics and Chaos* (Wiley, New York, 1987).
- [8] T. S. Parker and L. O. Chua, *Practical Numerical Algorithms for Chaotic Systems* (Springer-Verlag, Berlin, 1989).
- [9] G. Gouesbet, *Phys. Rev. A* **42**, 5928 (1990).
- [10] W. H. Press, B. P. Flannery, S. A. Teukolsky, and W. T. Vetterling, *Numerical Recipes, The Art of Scientific Computing* (Cambridge University Press, Cambridge, England, 1986).
- [11] M. Casdagli, *Physica D* **35**, 335 (1989).
- [12] J. D. Farmer and J. J. Sidorowich, *Phys. Rev. Lett.* **59**, 845 (1987).
- [13] M. Barnsley, *Fractals Everywhere* (Academic, New York, 1988).
- [14] E. Ott, W. D. Withers, and J. A. Yorke, *J. Stat. Phys.* **36**, 845 (1982).